Since January 2020 Elsevier has created a COVID-19 resource centre with free information in English and Mandarin on the novel coronavirus COVID-19. The COVID-19 resource centre is hosted on Elsevier Connect, the company's public news and information website.

Analytica Chimica Acta 1229 (2022) 340343

Contents lists available at ScienceDirect

Analytica Chimica Acta

journal homepage: www.elsevier.com/locate/aca

Real-time monitoring of isothermal nucleic acid amplification on a smartphone by using a portable electrochemical device for home-testing of SARS-CoV-2

Qi Li [a,1], Yang Li [a,1], Qian Gao [a], Chao Jiang [a], Qingwu Tian [a,**], Cuiping Ma [b], Chao Shi [a,*]

[a] Qingdao Nucleic Acid Rapid Testing International Science and Technology Cooperation Base, College of Life Sciences, Department of Pathogenic Biology, School of Basic Medicine, Department of Clinical Laboratory, the Affiliated Hospital of Qingdao University, Qingdao University, Qingdao, 266071, PR China
[b] Shandong Provincial Key Laboratory of Biochemical Engineering, Qingdao Nucleic Acid Rapid Detection Engineering Research Center, College of Marine Science and Biological Engineering, Qingdao University of Science and Technology, Qingdao, 266042, PR China

HIGHLIGHTS

- A portable electrochemical device was developed for home-testing of SARS-CoV-2.
- Testing carried out via this device could be real-time monitored on smartphones.
- Results could be automatically judged by preset criteria in microcontroller unit.
- Users can choose to save the results locally or share them on the cloud.
- The sensitivity of this device was comparable to fluorescence optical components.

GRAPHICAL ABSTRACT

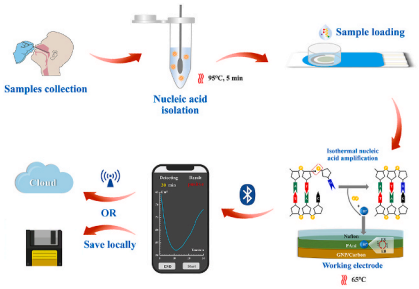

ARTICLE INFO

Keywords:
Real-time monitoring
Electrochemical detection
Isothermal nucleic acid amplification
pH-sensitive potentiometric sensor
Smartphone

ABSTRACT

Home-testing of SARS-CoV-2 is an ideal approach for controlling the pandemic of COVID-19 and alleviating the shortage of medical resource caused by this acute infectious disease. Herein, a portable device that enables real-time monitoring of isothermal nucleic acid amplification tests (INAATs) through the electrochemistry method was fabricated for home-testing of SARS-CoV-2. First, a disposable plug-and-play pH-sensitive potentiometric sensor that matches this electrochemical INAATs (E-INAATs) device was designed to allow the label-free pH sensing detection of nucleic acid. By applying Nafion film on the polyaniline-based working electrode, this sensor exhibited an excellent linear potentiometric response to pH value in the range of 6.0–8.5 with a slope of −37.45 ± 1.96 mV/pH unit. A Bluetooth module was integrated into this device to enable the users real-time monitoring INAATs on their smartphones at home. Moreover, by presetting criteria, the detection results could be automatically judged by the device to avoid human errors. Finally, the utility of this E-INAATs device was demonstrated by detecting the presence of SARS-CoV-2 nucleocapsid protein gene in artificial samples with a sensitivity of 2×10^2 copies/test within 25 min, which was comparable with fluorescence and colorimetric assay. This portable, easy-operated, sensitive, and affordable device is particularly desirable for the full integration of

* Corresponding author.
** Corresponding author.
E-mail addresses: tiantqw@126.com (Q. Tian), sc169@163.com (C. Shi).
[1] These two authors contributed equally to this work.

https://doi.org/10.1016/j.aca.2022.340343
Received 19 March 2022; Received in revised form 27 July 2022; Accepted 31 August 2022
Available online 7 September 2022

household SARS-CoV-2 detection products and will open a new prospect for the control of infectious diseases via electrochemical NAATs.

Abbreviation list

NAATs	Nucleic acid amplification tests
INAATs	Isothermal nucleic acid amplification tests
E-INAATs	Electrochemical isothermal nucleic acid amplification tests
PCR	Polymerase chain reaction
LAMP	Loop-mediated isothermal amplification
PAni	Polyaniline
PCB	Printed circuit board
MCU	Microcontroller unit
SCM	Single-chip microcomputer
ADC	Analog-to-digital converters
SEM	Scan electron microscope
NTC	No template control

1. Introduction

Due to the shortage of public healthcare resources caused by the prevalence of COVID-19 worldwide [1,2], the reliable and sensitive self-testing of SARS-CoV-2 at home has become an important approach to deal with the global health crisis caused by this acute infectious disease. Although the test strips based on antigen tests have been widely used for at-home SARS-CoV-2 detection at present, negative results of strips need to be interpreted with caution due to the number of false negative tests, with a broad variation in virus concentration [3]. Compared with immunoassays like antigen tests, nucleic acid amplification tests (NAATs) are considered more powerful tools for pathogen detection [4], among which real-time fluorescence polymerase chain reaction (PCR) has been employed as the gold standard for SARS-CoV-2 detection due to its excellent sensitivity and specificity [5,6]. However, conventional PCR normally requires bulky and costly thermal cycle and sophisticated fluorescence optical components, leading to the application of this approach only centralized in medical laboratories [7], while being less suitable for home-testing or in primary medical units lacking funding, which would not benefit to prevent COVID-19 transmission timely or control this acute infectious disease *in situ* [8]. Therefore, the development of portable devices integrated with NAATs that enables at-home self-diagnosis of COVID-19 is of great significance to prevent and control this disease.

Compared with the thermal cycling procedures, isothermal nucleic acid amplification technologies, e.g., loop-mediated isothermal amplification (LAMP), are more desirable for developing integrated portable NAATs devices, since these means simplify the thermal management of the device while suitable for visible colorimetric detection [9,10]. Besides isothermal nucleic acid amplification technologies, electrochemical methods have also been considered as a promising alternative to fluorescent-based optical sensing detection methods and more favorable to enable miniaturization and simplification of the detection devices [11–13]. Therefore, devices combining isothermal nucleic acid amplification technologies and electrochemical detection have been broadly reported for NAATs-based pathogen detection [14–16]. However, most of these reported systems are endpoint detecting systems or need bulky and expensive instruments (e.g., electrochemical workstation) to accomplish real-time monitoring, making them time-consuming and undesirable for home-testing. Moreover, the traditional detection systems generally could not connect to the internet and upload the data to the cloud, leading to them hard to contribute to COVID-19 prevention and control via the internet of things (IoT), a novel approach enables the healthcare system to properly monitor COVID-19 patients through big data analysis [17,18]. Despite some novel handheld devices for SARS-CoV-2 detection having been proposed [19], these devices are normally disposable, leading to high testing expenses.

In this present work, a portable electrochemical INAATs (E-INAATs) device combining the function of real-time monitoring and label-free electrochemical detection, as well as a matched plug-and-play disposable pH-sensitive potentiometric sensor were designed and fabricated. Nafion film was applied on the polyaniline (PAni)-based working electrode of the pH-sensitive potentiometric sensor to provide stable continuous voltage signals, whose potentiometric responses to pH value, temperature, and pyrophosphate were assessed. A Bluetooth module was integrated into this device to achieve real-time monitoring of the INAATs on a smartphone, instead of relying on bulky instruments. Finally, the performance of the INAATs device was evaluated by detecting nucleocapsid protein gene (N gene) of SARS-CoV-2 in simulated SARS-CoV-2 positive nasopharyngeal swabs.

2. Material and methods

2.1. Materials and reagents

DropSens 110 screen-printed electrode was purchased from Metrohm (China) Co., Ltd (Beijing, China). Printed circuit board (PCB) was obtained from JALC Technology Development Co., Ltd (Shenzhen, China). The heating module and Bluetooth (HC05) module were obtained from Yuanqin Biotech Co., Ltd (Shenzhen, China) and Alientek Co., Ltd (Guangzhou, China), respectively. Aniline was purchased from Macklin Biochemical Co., Ltd (Shanghai China). Nafion was purchased from DuPont China Holding Co., Ltd Shanghai Branch (Shanghai, China). Fluorescence/colorimetric LAMP detection kits for SARS-CoV-2 (ID: JM001), RS5 nucleic acid releaser (ID: JM103-3), and *Escherichia coli* O157:H7 strain (ATCC 35150) were provided by Navid Biotech Co., Ltd (Qingdao, China). SARS-CoV-2 N gene pseudovirus was purchased from Fubio Biological Technology Co., Ltd (Shanghai, China). The SARS-CoV-2 pseudovirus was composed with RNA molecular containing partial sequence of SARS-CoV-2 nucleocapsid protein gene and coat protein of the virus that cannot infect humans. DNA ladder (2000 bp) was purchased from Thermo Fisher Scientific (China) Co., Ltd (Shanghai, China). All the other chemicals and reagents were of analytical grade.

2.2. Design and fabrication of E-INAATs device and pH-sensitive potentiometric sensor

The E-INAATs device mainly consists of an STM32F103 single-chip microcomputer (SCM), a voltage amplifier, a thermostatic heating module, a Bluetooth module, all of which were integrated on a PCB (4 cm × 4 cm) and powered by a rechargeable lithium-ion battery (3.3 V, 500 mAh), as well as a disposable plug-and-play pH-sensitive potentiometric sensor (Fig. 1A). The circuit assembly of the device was illustrated in Fig. S1 and Table S1. Particularly, the STM32F103 SCM is embedded with an ARM-based 32-bit microcontroller unit (MCU) and two 12-bit analog-to-digital converters (ADC), whose voltage accuracy is 0.02 mV. The pH-sensitive potentiometric sensor is a three-electrode system containing gold nanoparticles (GNP)/carbon working electrode, a silver reference electrode, and a carbon counter electrode, which were screen printed on a ceramic substrate.

To realize the conversion of pH value to electrical signal and real-time monitoring of the signal, the working and reference electrodes of the sensor were modified according to a previous report with some

modifications [20] (Fig. 1B). Specifically, PAni electrodeposition on working electrode was performed with 40 μL 0.1 M aniline solution in 1 M HCl via 12 cyclic voltammetry (CV) from −0.2 V to 1.0 V vs. Ag/AgCl at 0.1 V/s. The working electrode was dried in a baking oven at 65 °C for 5 min after the residual liquid was removed, followed by washed with deionized water and air-dried. To enhance the stability of the sensor, 1 μL of 1 wt% Nafion solution (diluted from 5 wt% Nafion solution with ethanol) was dropped on the PAni film deposited on the working electrode and air-dried for 1 h. The reference electrode was sealed by polyethylene film in prior to the application of Nafion film to avoid the solution splashing on it. The working electrode was then washed with deionized water and air-dried. During the period of air-drying, a polyvinyl butyral (PVB)-based membrane was prepared to improve the stability of the reference electrode [21]. Briefly, 78.1 mg PVB and 50 mg NaCl were completely dissolved in 1 mL methanol via ultrasonic vibration in an AJT instrument ultrasonic bath at 75 Hz for 30 min. Subsequently, the protective polyethylene film was removed, followed by drop-casting 2.5 mL PVB-based membrane onto the reference electrode area, which was desiccated overnight. Finally, a short polypropylene pipe was sticked enclosing the electrodes by epoxy resin to perform as reaction vessel, and the sensor was ready to be used after stay at room temperature for 12 h.

2.3. Characterization of the pH-sensitive potentiometric sensor

To observe the changes of the working electrode substrate after coating with Nafion film, both the PAni- and PAni/Nafion-based working electrodes were observed by a scan electron microscope (SEM, VEGA3, TESCAN, Brno-Kohoutovice, Czech Republic). In addition, the substrate of these working electrodes was further observed by SEM after dropping 25 μL Tris-EDTA (TE) buffer (containing 1 M Tris and 0.5 M EDTA, pH = 8.5) on them and heating at 65 °C for 30 min. The potentiometric response of the sensor to pH value was measured by adding TE buffer with the pH value from 6.0 to 8.5 into the reaction vessel enclosing the electrodes. The potentiometric response was real-time monitored by using the potential-time program of a potentiostat. Finally, the influences of reaction temperature and pyrophosphate content were also determined. Specifically, TE buffer (pH = 8.5) was added into the reaction vessel, the potentiometric response was measured at six different temperatures (20 °C, 30 °C, 40 °C, 50 °C, 60 °C and 65 °C) to evaluate the influence of reaction temperature, while the change of potentiometric response when $Na_4P_2O_7$ solution of various concentration (10^{-7} M, 10^{-6} M, and 10^{-5} M) added into the reaction vessel were recorded to assess the influence of pyrophosphate.

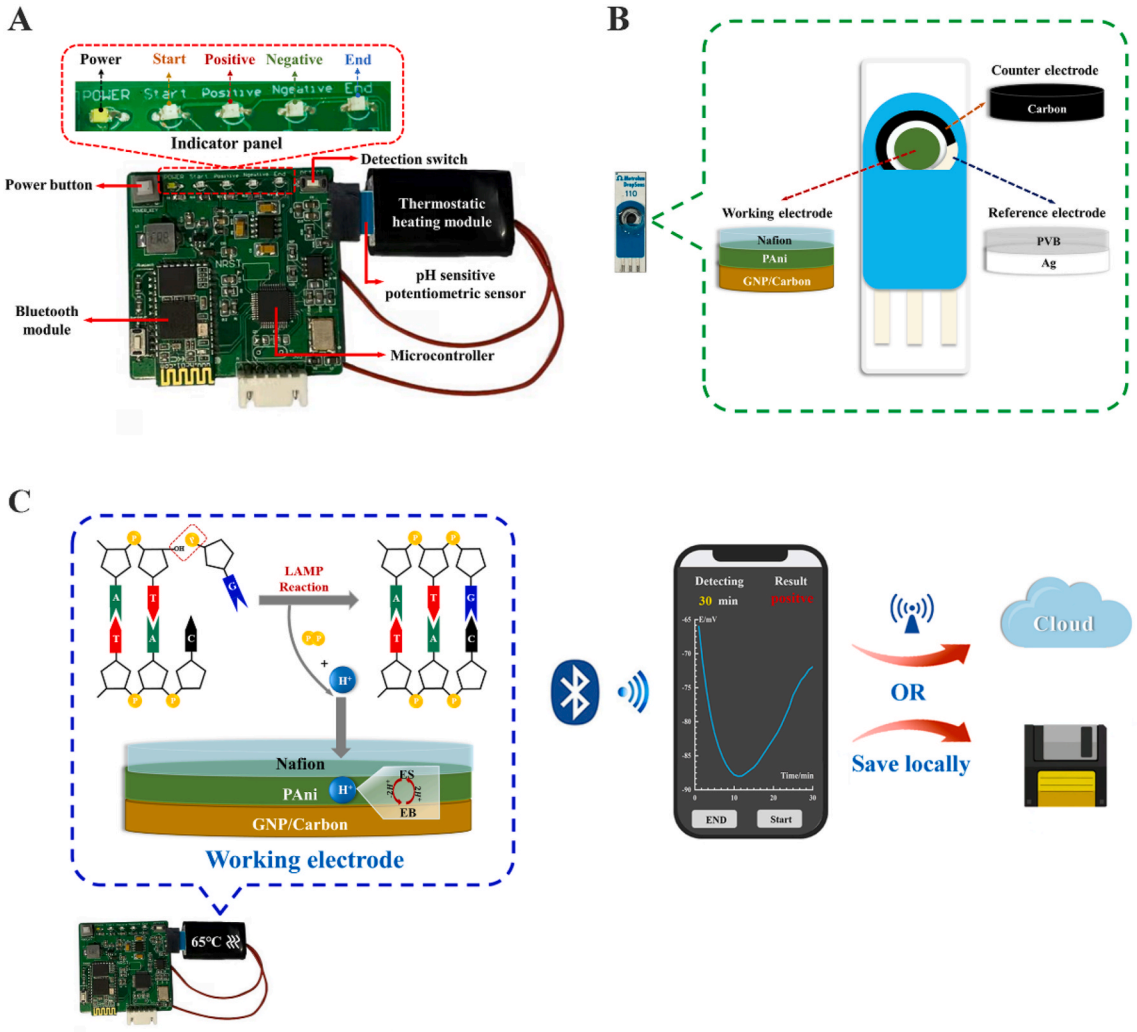

Fig. 1. Components of the E-INAATs device and its operating principle. (A) Schematic of the integrated E-INAATs device. Red dash line framed the indicator LED lights. (B) Schematic of the electrodes of PAni/Nafion-based pH-sensitive potentiometric sensor. (C) Schematic of the mechanism for proton release during LAMP reactions as well as the response of PAni to pH or potential changes. The reactions could be real-time monitored on a smartphone, which allow the users saving the results locally or uploading them to the cloud.

2.4. Real-time monitoring of LAMP assays by the E-INAATs device

In this study, LAMP assays were employed for target nucleic acid detection, the reaction process of which were real-time monitored by the E-INAATs device. Specifically, 25 μL of LAMP reaction mixtures were first prepared by mixing 23 μL of LAMP master mix and 2 μL relevant templates according to the manufacturer's instruction of fluorescence/colorimetric LAMP detection kits for SARS-CoV-2. Then the prepared mixtures were loaded into the reaction vessel of the pH-sensitive potentiometric sensor, followed by covered the vessel with a small piece of polyethylene film. Subsequently, the sensor was connected to the device and inserted into the thermostatic heating module, and the LAMP assays were operated at 65 °C for 30 min. During the LAMP assays process, H^+ were continuously produced with the extension of the oligonucleotide chain. The sensor would monitor the H^+ content in real-time by the equilibrium between the two partially oxidized forms, deprotonated emeraldine base (EB) and protonated emeraldine salt (ES), of the PAni in the working electrode (Fig. 1C) [22], and convert it to a voltage signal in the range of −100 mV ~ −20 mV, which was then amplified to 300 mV–2700 mV by the voltage amplifier and transmitted to the SCM. The SCM measured potentiometric and recorded the signal from the sensor every 100 ms. After the treatment of average filtrating and median filtrating to the signal, final data were obtained every 6 s, which was then stored in the storage unit of the MCU and analyzed based on the preset criteria (Fig. S2). Specifically, the results are determined as positive when the value of any six of ten consecutive-points are 0.1 mV greater than the previous one 10 min after the tests start, while the results are determined as negative when the value of any twelve of twenty consecutive-points are 0.1 mV less than the previous one 20 min after the test start or none of the above conditions are met 30 min after the tests start. According to the analysis results, the MCU controlled the indicator LED lights exhibiting relevant detection results. In addition, the analysis results were also transmitted to the Bluetooth module, by using which the wireless communication could interface the output to a Bluetooth-enabled smartphone in real-time. Finally, an App was developed by using App Inventor (Fig. S3) to allow the users to read the detection results on their smartphones (Video "Positive" and Video "Negative"), and provide the users options of saving the detection results locally or uploading them to the cloud (Fig. 1C).

Supplementary video related to this article can be found at https://doi.org/10.1016/j.aca.2022.340343

Besides electrochemical LAMP assay, fluorescence and colorimetric LAMP assays were also carried out with the same samples as templates for comparison. Real-time fluorescence LAMP assays were tested by the CFX Connect™ Real-Time System (BioRad, CA, USA) at 1-min intervals. The colorimetric LAMP assays were carried out in a dry bath, and the absorbance of the reaction systems at 544 nm was measured by a NanoDrop™ One Microvolume UV–Vis Spectrophotometer (Thermo Scientific™, MA, USA) at 10-min intervals. Moreover, the visible color changes of the reaction systems were also recorded every 10 min.

2.5. Detection of SARS-CoV-2 in artificial samples by E-INAATs device

Artificial samples of simulated SARS-CoV-2 positive nasopharyngeal swabs were employed as targets to evaluate the performance of the E-INAATs device. Specifically, volunteers' throat or nasal was swabbed by nasopharyngeal swabs, then 50 μL SARS-CoV-2 pseudovirus suspensions at various concentrations (10^8, 10^7, 10^6, 10^5 copies/mL) were dropped on these swabs to prepare simulated SARS-CoV-2 positive nasopharyngeal swabs. The nucleic acid of the artificial samples was simply isolated by immersing the swabs in 450 μL RS5 nucleic acid releaser, which was then heated at 95 °C for 5 min. Then 2 μL crude nucleic acid extracts were directly mixed into 23 μL LAMP master mix and loaded into the reaction vessel of the pH-sensitive potentiometric sensor subsequently (approximately 2×10^4, 2×10^3, 2×10^2 and 2×10^1 copies in each test).

3. Results and discussion

3.1. Substrate morphology of the working electrode

In this study, the pH-sensitive potentiometric sensor was employed to achieve label-free measurement of this device since the sensors depend on DNA-intercalative electroactive molecules (e.g., methylene blue) as indicators suffering from low signal resolution due to the weak binding affinity of these molecules to amplicons [23]. The disposable plug-and-play pH-sensitive potentiometric sensor matched the E-INAATs device was designed to avoid false-positive results caused by the sample residual on the reused sensor. Moreover, using this design, the device could be multiple reuses through replacing the sensor, which would reduce detection costs. Despite some electrodes based on noble metal were reported possessing excellent sensitivity, such as Pt/IrO_x and Ir/IrO_x electrodes [24], they are not suitable for the preparation of plug-and-play sensors due to the high expense. Therefore, PAni-based working electrode was first employed for pH-sensitive potentiometric sensor fabrication, since PAni is a widely used low-cost pH-sensitive material that subjects to both RedOx and protonation−deprotonation [25–27]. To validate the stability of the device integrated with this sensor, SARS-CoV-2 pseudovirus suspensions with concentrations from 10^7 to 10^3 copies/mL were employed as targets (approximately 2×10^4 to 2×10^0 copies in each test). As shown in Fig. S4A, the potentiometric response of the E-INAATs device integrated with the PAni-based sensor failed to exhibit a significant correlation with the target concentration. Even the group of no template control (NTC) exhibited a strong potentiometric response. We supposed that the continuous heating during LAMP assays would weaken the affinity between PAni and the working electrode, which might lead to the spalling of the PAni deposited on the working electrode and suffering the risk of failure. To verify our conjecture, the substrate of the PAni-based working electrode was observed by SEM after heating TE buffer on its surface at 65 °C for 30 min. Compared with the electrode without heating treatment (Fig. S4B a), the substrate of the heated electrode exhibited obvious crack (Fig. S4B b), which may lead to the spalling of the PAni and influence signal collection. To improve the stability of the E-INAATs device, Nafion was employed to coat on the working electrode of the sensor since this ion exchange membrane material could enhance affinity between PAni and working electrode besides improving its conductivity [28,29]. The SEM images showed that despite the morphology of the electrode substrate exhibited no obvious change after coating the Nafion film (Fig. S4B c), the crack no longer appeared on the substrate after heating (Fig. S4B d), demonstrating Nafion film could indeed prevent the crack of the substrate, as well as the spalling of the PAni during INAATs, which would improve the stability of the sensor. This PAni/Nafion-based working electrode was more desirable for constructing pH-sensitive potentiometric sensors that would provide precise detection results.

3.2. Potentiometric response of the E-INAATs device

According to previous reports, the change in pH value is normally around 2.5 units when the LAMP reaction occurred in a non-buffered solution [30]. Since the pH value of the LAMP master mix used in this study is around 8.5, the potentiometric response of the E-INAATs device was characterized by using TE buffer with a pH value from 6.0 to 8.5. Normally the relationship between the potential response of pH sensing electrodes and the pH value follows the Nernst Equation [31]. As shown in Fig. 2A and B, our pH sensing electrode showed a sub-Nernstian response with a slope of −37.45 ± 1.96 mV/pH within the pH range of 6.0–8.5, which might be attributed to that one or two electrons were involved in the combination of H^+ ion exchange and electronic transfer [32]. Despite the pH sensing electrode might show lower sensitivity than

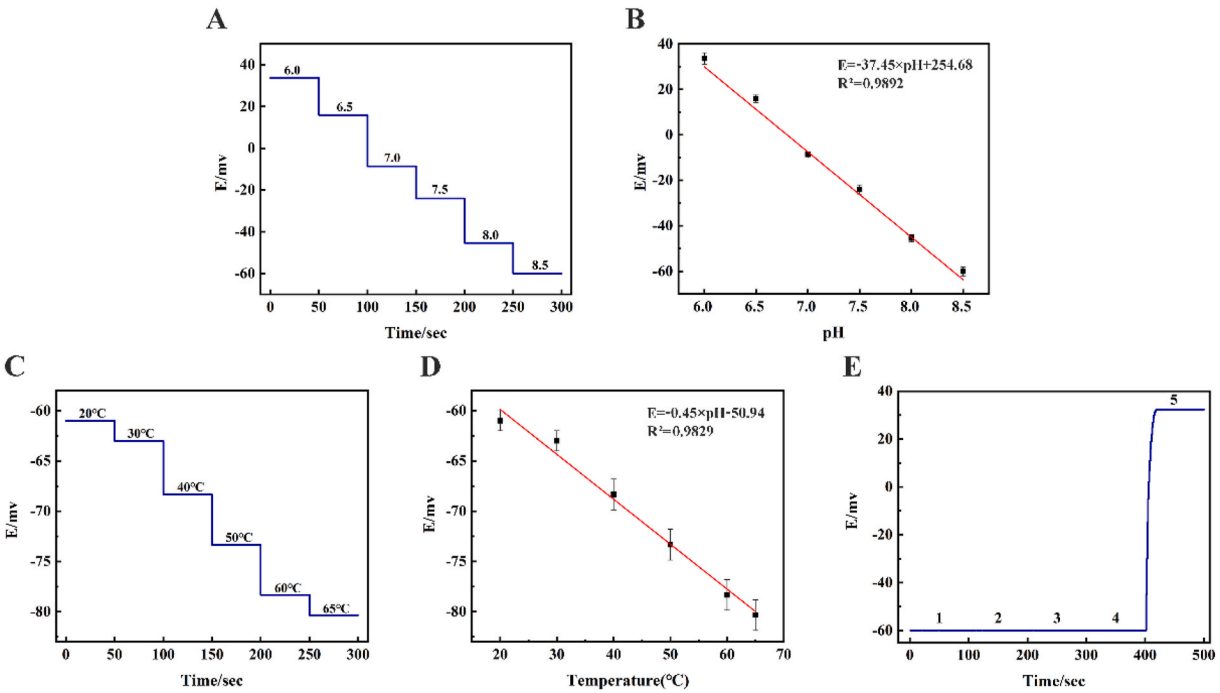

Fig. 2. (A) Potential-time potentiometric response of E-INAATs device in the pH value ranging from 6.0 to 8.5 at room temperature. (B) A linear relationship between the potentiometric response and pH value. (C) Potential-time potentiometric response of E-INAATs device in TE buffer (pH = 8.5) at the temperature ranging from 20 °C to 65 °C. (D) A linear relationship between the potentiometric response and temperature. (E) Interference assay of pyrophosphate to the E-INAATs device. 1–5 represented TE buffer with a pH value of 8.5, 10^{-7} M, 10^{-6} M, 10^{-5} M pyrophosphate TE buffer (pH 8.5) solution, and TE buffer with a pH value of 6.0, respectively. Error bars represent the standard deviations of three independent measurements.

those with Nernstian response [33], the potentiometric response of the electrode exhibited a significant linear relationship to the pH value in this range with a corresponding coefficient (R^2) of 0.9892, demonstrating the excellent stability of the E-INAATs device. Besides pH value, the potentiometric response of the E-INAATs device was also negative linearly related to the reaction temperature in the range of 20 °C–65 °C (Fig. 2C and D). Despite that the reaction temperature was an important factor affecting potentiometric response, the results showed that the potentiometric response was stable at a constant reaction temperature, thus the influence of temperature on potentiometric responses would not substantially affect the real-time monitoring of pH value for LAMP assays and other INAATs, since these reactions are carried out at a constant temperature in the E-INAATs device. In addition, since pyrophosphate is produced with H^+, the influence of pyrophosphate on potentiometric response was also evaluated. During the extension of the oligonucleotide chain, one H^+ and one pyrophosphate are released from the sugar-phosphate backbone for every new phosphodiester bond formed, the yield of H^+ and pyrophosphate should be 1:1 during NAATs theoretically [34], which means approximately 10^{-6} M pyrophosphate should be yielded when the pH value decreased from 8.5 to 6.0. As shown in Fig. 2E, the potential scarcely changed after $Na_4P_2O_7$ solutions with the concentration of 10^{-7} M, 10^{-6} M, and 10^{-5} M were added on the sensor, the range of change was far less than that caused by the pH value decreasing from 8.5 to 6.0 (approximately 90 mV), indicated that the production of pyrophosphate could hardly affect potentiometric response during INAATs. Moreover, since the content of other ions (e.g. Na^+, K^+, Cl^-, SO_4^{2-} and NO_3^-) in the system barely changed during LAMP assays, their influences were also nearly ignorable [8]. In all, the E-INAATs device is highly selective for H^+ detection and is ideal for real-time pH monitoring in electrochemical LAMP assays.

3.3. Detection of SARS-CoV-2 in artificial samples by E-INAATs device

To further evaluate the feasibility and the sensitivity of the E-INAATs device on SARS-CoV-2 detection in artificial samples, simulated SARS-CoV-2 positive samples prepared by spiking various concentrations of SARS-CoV-2 pseudovirus in nasopharyngeal swabs were employed as targets, whose nucleic acids were first simply and ultrafast isolated by thermal lysis method. Considering that the potential drifting that occurred during the LAMP assay would affect the detection results, we normalized the potentials of all the electrodes of the pH-sensitive potentiometric sensor by subtracting that of the negative sample set as a baseline to minimize this effect [9]. Fig. 3A showed that the presence of SARS-CoV-2 pseudovirus (no less than 10^6 copies/mL, approximately 2×10^2 copies/test) would cause a significant increase in the potentials of the pH-sensitive potentiometric sensor within 25 min. The sharp decrease of the potentiometric during the very beginning of electrochemical LAMP assay should be attributed to the rapid rise of temperature. The amplicons shown in the agarose gel electrophoresis image demonstrated LAMP reactions were carried out, the H^+ produced during which process was the main cause of potentials increase [35]. These potential curves also exhibited that potentiometric response was highly related to the concentration of SARS-CoV-2 pseudovirus. Specifically, the higher concentration of SARS-CoV-2 pseudovirus could cause earlier accumulation of H^+ and the increase of the potential, and the potential at the plateau stage was higher as well. The results also demonstrated that the reverse transcription process required for RNA targets detection would not affect the potentiometric response of the sensor, making the E-INAATs device suitable for one-step detection of RNA targets. Besides electrochemical LAMP assays, fluorescence and colorimetric LAMP assays were also carried out for comparison, the results showed that the electrochemical LAMP assays carried out by using E-INAATs device exhibited a comparable sensitivity and time consumption with fluorescence LAMP assays (Fig. 3B), while had a better performance than colorimetric LAMP assays in time consumption, as colorimetric LAMP assay required more than 50 min (Fig. 3C). Despite the results of colorimetric LAMP can also be simply observed by naked eyes, the color changes are sometimes hard to determine when the concentration of

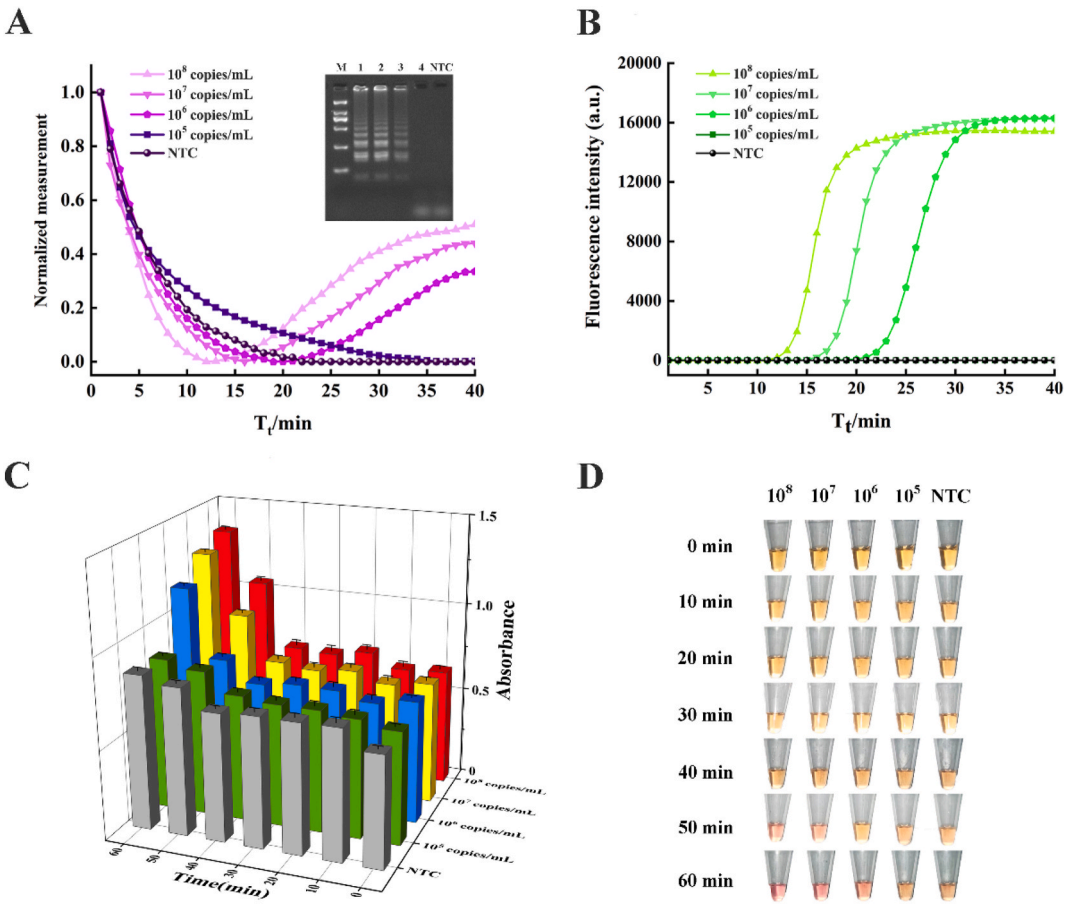

Fig. 3. (A) Normalized potential-time curves of electrochemical LAMP assays for the artificial samples containing various concentrations of SARS-CoV-2 pseudovirus in E-INAATs device. Inset is the agarose gel electrophoresis images of LAMP products of relevant artificial samples. M represented DNA ladder (2000 bp). 1–4 represented artificial nasopharyngeal swabs prepared with 10^8, 10^7, 10^6, and 10^5 copies/mL SARS-CoV-2 pseudovirus suspensions, respectively. NTC represented no template control. (B) Fluorescence curves of the LAMP reaction for the same artificial samples. (C) Absorbance of the colorimetric LAMP reaction systems for the same artificial samples. (D) Visible color change of the colorimetric LAMP reaction systems with time for the same artificial samples (unit: copies/mL).

target nucleic acid is closed to the limit of detection (Fig. 3D). In contrast, the device could judge the detection results and present them to the users on smartphones or its indicator panel by the preset threshold in MCU, rather than judging the results by the users themselves, which would avoid the human errors. Although some automated colorimetric detection devices could also achieve the real-time monitoring of INAATs and judging the detection results, even some of which have been proved to have higher sensitivity than electrochemical detection devices, the high expense of the required sophisticated optics might restrict their extension application [36–38]. Besides SARS-CoV-2 pseudovirus, another pathogen, *Escherichia coli* O157:H7 was also employed as a target to evaluate the performance of E-INAATs device on the detection of DNA targets. As expected, this E-INAATs device could detect as low as 2×10^2 CFU *E. coli* O157:H7 (Fig. 4A), which also showed comparable sensitivity with fluorescence (Fig. 4B) and colorimetric LAMP assays (Fig. 4C and D), demonstrating this device is suitable for the detection of other pathogens. More importantly, the LAMP assays could be real-time monitored by observing the potential-time curves displayed on the smartphone, which allows the users to determine positive samples before the end of entire LAMP assays and deal with these samples timely. Furthermore, the detection data could be uploaded to the cloud and shared on IoT, making this E-INAATs device able to contribute to COVID-19 prevention and control via this novel efficient approach besides enabling simple, rapid, low-cost, and label-free electrochemical nucleic acid detection.

4. Conclusion

In this present study, a portable electrochemical INAATs device and a disposable pH-sensitive potentiometric sensor matched this device were designed and fabricated. By applying a Nafion film on the working electrode, the disposable pH-sensitive potentiometric sensor provided a stable continuous potentiometric measurement of the pH value and showed a sub-Nernstian response with a slope of -37.45 ± 1.96 mV/pH unit, which is critical to ensure that the device accurately monitors INAATs in real-time. Moreover, this E-INAATs device has been successfully demonstrated to exhibit a comparable sensitivity with the fluorescence and colorimetric assays as well as less time consumption than the colorimetric assays for nucleic acid target isolated from artificial samples. In addition to simply reading out the detection results through the indicator LED lights, this device also allows the users real-time monitoring the INAATs on their smartphones without the help of bulky sophisticated instruments and provides the users the options of saving the detection results locally or uploading them to the cloud, which is convenient for personal health management. In summary, this proposed portable device successfully realizes the combination of molecular biology, electrochemistry, and instrumental science, and provides a simple, efficient, and low-cost approach for ultrafast self-testing of pathogens like SARS-CoV-2 at home, as well as ideas for the development of portable full integration medical detection devices fighting infectious diseases.

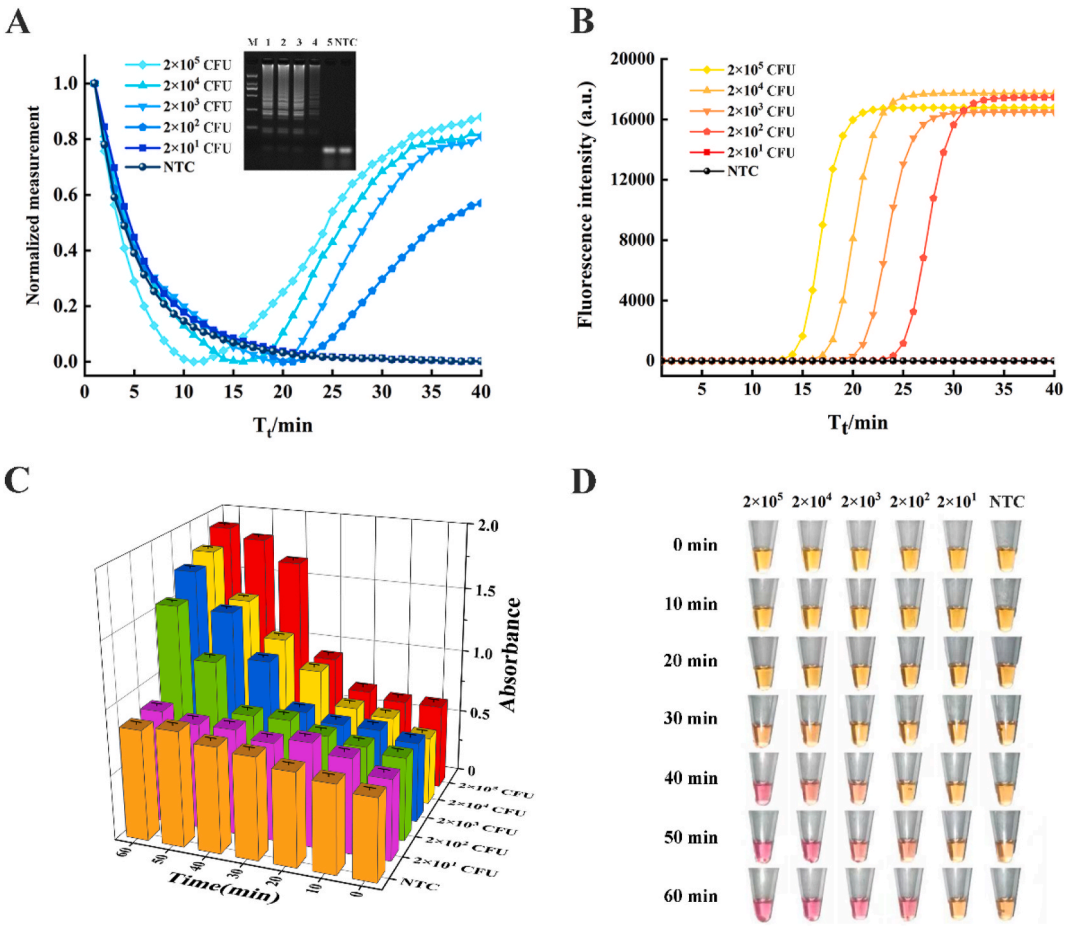

Fig. 4. (A) Normalized potential-time curves of electrochemical LAMP assays for *E. coli* O157:H7 samples in E-INAATs device. Inset is the agarose gel electrophoresis images of LAMP products of relevant samples. M represented DNA ladder (2000 bp). 1–5 represented the reaction systems containing 2×10^5, 2×10^4, 2×10^3, 2×10^2, and 2×10^1 CFU *E. coli* O157:H7, respectively. NTC represented no template control. (B) Fluorescence curves of the LAMP reaction for the same samples. (C) Absorbance of the colorimetric LAMP reaction systems for the same samples. (D) Visible color change of the colorimetric LAMP reaction systems with reaction time for the same samples (unit: CFU).

Ethics approval

All sample collection work and tests were conducted with the volunteers' consent and approved by the authorized Human Health and Ethics Committee of the Affiliated Hospital of Qingdao University, and all operations were conducted following relevant guidelines and regulations.

Authors' contributions

Qi Li, Qian Gao, and Chao Jiang performed the experiments; Yang Li and Qi Li analyzed the data; Qi Li designed the PCB and the smartphone App. Chao Shi, Yang Li, Cuiping Ma, and Qingwu Tian designed the experimental scheme; Yang Li and Qi Li wrote the manuscript, and all authors contributed to the writing of the paper, had primary responsibility for the final content, and read and approved the final manuscript.

Declaration of competing interest

The authors declare that they have no known competing financial interests or personal relationships that could have appeared to influence the work reported in this paper.

Data availability

Data will be made available on request.

Acknowledgment

We highly appreciate the financial support of the Major Scientific and Technological Innovation Projects of Shandong Province (2022SFXGFY01), the Science and Technology Benefiting the People Demonstration Project of Qingdao (22-2-7-smjk-2-nsh), and the Key Project of Shandong Province Natural Science Foundation (ZR2020KH030).

Appendix A. Supplementary data

Supplementary data to this article can be found online at https://doi.org/10.1016/j.aca.2022.340343.

References

[1] K. Kotfis, S. Williams Roberson, J.E. Wilson, W. Dabrowski, B.T. Pun, E.W. Ely, COVID-19: ICU delirium management during SARS-CoV-2 pandemic, Crit. Care 24 (1) (2020) 176.

[2] T.W. Farrell, L. Francis, T. Brown, L.E. Ferrante, E. Widera, R. Rhodes, T. Rosen, U. Hwang, L.J. Witt, N. Thothala, S.W. Liu, C.A. Vitale, U.K. Braun, C. Stephens, D. Saliba, Rationing limited healthcare resources in the COVID-19 era and beyond: ethical considerations regarding older adults, J. Am. Geriatr. Soc. 68 (6) (2020) 1143–1149.

[3] M. Möckel, V.M. Corman, M.S. Stegemann, J. Hofmann, A. Stein, T.C. Jones, P. Gastmeier, J. Seybold, R. Offermann, U. Bachmann, T. Lindner, W. Bauer, C. Drosten, A. Rosen, R. Somasundaram, SARS-CoV-2 antigen rapid immunoassay for diagnosis of COVID-19 in the emergency department, Biomarkers 26 (3) (2021) 213–220.
[4] C. Yang, Y. Li, J. Deng, M. Li, C. Ma, C. Shi, Accurate, rapid and low-cost diagnosis of Mycoplasma pneumoniae via fast narrow-thermal-cycling denaturation bubble-mediated strand exchange amplification, Anal. Bioanal. Chem. 412 (30) (2020) 8391–8399.
[5] B. Böger, M.M. Fachi, R.O. Vilhena, A.F. Cobre, F.S. Tonin, R. Pontarolo, Systematic review with meta-analysis of the accuracy of diagnostic tests for COVID-19, Am. J. Infect. Control 49 (1) (2021) 21–29.
[6] A.J. Colbert, D.H. Lee, K.N. Clayton, S.T. Wereley, J.C. Linnes, T.L. Kinzer-Ursem, PD-LAMP smartphone detection of SARS-CoV-2 on chip, Anal. Chim. Acta (2022), 339702.
[7] M.S. Han, J.H. Byun, Y. Cho, J.H. Rim, RT-PCR for SARS-CoV-2: quantitative versus qualitative, Lancet Infect. Dis. 21 (2) (2021) 165.
[8] Z. Xu, K. Yin, X. Ding, Z. Li, X. Sun, B. Li, R.V. Lalla, R. Gross, C. Liu, An integrated E-Tube cap for sample preparation, isothermal amplification and label-free electrochemical detection of DNA, Biosens. Bioelectron. 186 (2021), 113306.
[9] D. Gosselin, M. Gougis, M. Baque, F.P. Navarro, M.N. Belgacem, D. Chaussy, A.-G. l. Bourdat, P. Mailley, J. Berthier, Screen-printed polyaniline-based electrodes for the real-time monitoring of loop-mediated isothermal amplification reactions, Anal. Chem. 89 (19) (2017) 10124–10128.
[10] Y. Liu, B. Lu, Y. Tang, Y. Du, B. Li, Real-time gene analysis based on a portable electrochemical microfluidic system, Electrochem. Commun. 111 (2020), 106665.
[11] K. Hsieh, A.S. Patterson, B.S. Ferguson, K.W. Plaxco, H.T. Soh, Rapid, sensitive, and quantitative detection of pathogenic DNA at the point of care through microfluidic electrochemical quantitative loop-mediated isothermal amplification, Angew. Chem., Int. Ed. 51 (20) (2012) 4896–4900.
[12] P.J. Asiello, A.J. Baeumner, Miniaturized isothermal nucleic acid amplification, a review, Lab Chip 11 (8) (2011) 1420–1430.
[13] N. Izadi, R. Sebuyoya, L. Moranova, R. Hrstka, M. Anton, M. Bartosik, Electrochemical bioassay coupled to LAMP reaction for determination of high-risk HPV infection in crude lysates, Anal. Chim. Acta 1187 (2021), 339145.
[14] M.R. Gore, V.A. Szalai, P.A. Ropp, I.V. Yang, J.S. Silverman, H.H. Thorp, Detection of attomole quantities of DNA targets on gold microelectrodes by electrocatalytic nucleobase oxidation, Anal. Chem. 75 (23) (2003) 6586–6592.
[15] S. Liu, Y. Wang, S. Zhang, L. Wang, Exonuclease-catalyzed methylene blue releasing and enriching onto a dodecanethiol monolayer for an immobilization-free and highly sensitive electrochemical nucleic acid biosensor, Langmuir 33 (21) (2017) 5099–5107.
[16] H.-A. Rafiee-Pour, M. Behpour, M. Keshavarz, A novel label-free electrochemical miRNA biosensor using methylene blue as redox indicator: application to breast cancer biomarker miRNA-21, Biosens. Bioelectron. 77 (2016) 202–207.
[17] R.P. Singh, M. Javaid, A. Haleem, R. Suman, Internet of things (IoT) applications to fight against COVID-19 pandemic, Diabetes Metabol. Syndr. 14 (4) (2020) 521–524.
[18] A. Roberts, S. Mahari, D. Shahdeo, S. Gandhi, Label-free detection of SARS-CoV-2 Spike S1 antigen triggered by electroactive gold nanoparticles on antibody coated fluorine-doped tin oxide (FTO) electrode, Anal. Chim. Acta 1188 (2021), 339207.
[19] L.J. Donato, V.A. Trivedi, A.M. Stransky, A. Misra, B.S. Pritt, M.J. Binnicker, B. S. Karon, Evaluation of the Cue Health point-of-care COVID-19 (SARS-CoV-2 nucleic acid amplification) test at a community drive through collection center, Diagn. Microbiol. Infect. Dis. 100 (1) (2021), 115307.
[20] T. Guinovart, G. Valdés-Ramírez, J.R. Windmiller, F.J. Andrade, J. Wang, Bandage-based wearable potentiometric sensor for monitoring wound pH, Electroanalysis 26 (6) (2014) 1345–1353.
[21] T. Guinovart, G.A. Crespo, F.X. Rius, F.J. Andrade, A reference electrode based on polyvinyl butyral (PVB) polymer for decentralized chemical measurements, Anal. Chim. Acta 821 (2014) 72–80.
[22] C. Ge, N.R. Armstrong, S.S. Saavedra, pH-sensing properties of poly(aniline) ultrathin films self-assembled on indium-tin oxide, Anal. Chem. 79 (4) (2007) 1401–1410.
[23] F. Zhang, J. Wu, R. Wang, L. Wang, Y. Ying, Portable pH-inspired electrochemical detection of DNA amplification, Chem. Commun. 50 (61) (2014) 8416–8419.
[24] M. Tabata, Y. Katayama, F. Mannan, A. Seichi, K. Suzuki, T. Goda, A. Matsumoto, Y. Miyahara, Label-free and electrochemical detection of nucleic acids based on isothermal amplification in combination with solid-state pH sensor, Procedia Eng. 168 (2016) 419–422.
[25] J. Dong, W. Pan, J. Luo, R. Liu, Synthesis of inhibitor-loaded polyaniline microcapsules with dual anti-corrosion functions for protection of carbon steel, Electrochim. Acta 364 (2020), 137299.
[26] A. Soni, C.M. Pandey, S. Solanki, G. Sumana, Synthesis of 3D-coral like polyaniline nanostructures using reactive oxide templates and their high performance for ultrasensitive detection of blood cancer, Sensor Actuat. B Chem. 281 (2019) 634–642.
[27] R. Mažeikienė, G. Niaura, A. Malinauskas, Study of redox and protonation processes of polyaniline by the differential multiwavelength Raman spectroelectrochemistry, Spectrochim. Acta 221 (2019), 117147.
[28] F.B. Diniz, K.C.S. de Freitas, W.M. de Azevedo, Ion exchange properties of polyaniline: potentiometric measurements on membranes and coated wire electrodes, Electrochim. Acta 42 (12) (1997) 1789–1793.
[29] J.-S. Do, Y.-H. Chang, M.-L. Tsai, Highly sensitive amperometric creatinine biosensor based on creatinine deiminase/Nafion®-nanostructured polyaniline composite sensing film prepared with cyclic voltammetry, Mater. Chem. Phys. 219 (2018) 1–12.
[30] N. Jogezai, M.I. Shabbir, A hand-held device for rapid single tube detection of hepatitis-C virus, Anal. Methods-UK 10 (35) (2018) 4233–4241.
[31] Z. Xu, Q. Dong, B. Otieno, Y. Liu, I. Williams, D. Cai, Y. Li, Y. Lei, B. Li, Real-time in situ sensing of multiple water quality related parameters using micro-electrode array (MEA) fabricated by inkjet-printing technology (IPT), Sensor Actuat. B Chem. 237 (2016) 1108–1119.
[32] R. De Marco, B. Pejcic, Electrochemical impedance spectroscopy and X-ray photoelectron spectroscopy study of the response mechanism of the chalcogenide glass membrane iron(III) ion-selective electrode in saline media, Anal. Chem. 72 (4) (2000) 669–679.
[33] G.D.M. Madeira, H.J.N.P. Dias Mello, M.C. Faleiros, M. Mulato, Model improvement for super-Nernstian pH sensors: the effect of surface hydration, J. Mater. Sci. 56 (3) (2021) 2738–2747.
[34] S. Purushothaman, C. Toumazou, C.-P. Ou, Protons and single nucleotide polymorphism detection: a simple use for the Ion Sensitive Field Effect Transistor, Sensor Actuat. B Chem. 114 (2) (2006) 964–968.
[35] Y. Liao, J. Gao, W. Huang, R. Yuan, W. Xu, LAMP-H+-responsive electrochemical ratiometric biosensor with minimized background signal for highly sensitive assay of specific short-stranded DNA, Biosens. Bioelectron. 195 (2022), 113662.
[36] K. Yin, V. Pandian, K. Kadimisetty, X. Zhang, C. Ruiz, K. Cooper, C. Liu, Real-time colorimetric quantitative molecular detection of infectious diseases on smartphone-based diagnostic platform, Sci. Rep. 10 (1) (2020) 9009.
[37] G. Papadakis, A.K. Pantazis, N. Fikas, S. Chatziioannidou, V. Tsiakalou, K. Michaelidou, V. Pogka, M. Megariti, M. Vardaki, K. Giarentis, J. Heaney, E. Nastouli, T. Karamitros, A. Mentis, A. Zafiropoulos, G. Sourvinos, S. Agelaki, E. Gizeli, Portable real-time colorimetric LAMP-device for rapid quantitative detection of nucleic acids in crude samples, Sci. Rep. 12 (1) (2022) 3775.
[38] L.M. Diaz, B.E. Johnson, D.M. Jenkins, Real-time optical analysis of a colorimetric LAMP assay for SARS-CoV-2 in saliva with a handheld instrument improves accuracy compared with endpoint assessment, J. Biomol. Tech. 32 (3) (2021) 158–171.